1. Björklund A, Lindvall O (2000) Cell replacement therapies for central nervous system disorders. *Nat Neurosci* 3:537–544.
2. Okano H (2002) Stem cell biology of the central nervous system. *J Neurosci Res* 69: 698–707.
3. Lindvall O, Kokaia Z, Martinez-Serrano A (2004) Stem cell therapy for human neurodegenerative disorders—how to make it work. *Nat Med* 10 (Suppl):S42–S50.
4. Martino G, Pluchino S (2006) The therapeutic potential of neural stem cells. *Nat Rev Neurosci* 7:395–406.
5. Lindvall O, Kokaia Z (2006) Stem cells for the treatment of neurological disorders. *Nature* 441:1094–1096.
6. Gage FH (2000) Mammalian neural stem cells. *Science* 287:1433–1438.
7. Wichterle H, Lieberam I, Porter JA, Jessell TM (2002) Directed differentiation of embryonic stem cells into motor neurons. *Cell* 110:385–397.
8. Watanabe K, et al. (2005) Directed differentiation of telencephalic precursors from embryonic stem cells. *Nat Neurosci* 8:288–296.
9. Sonntag KC, et al. (2007) Enhanced yield of neuroepithelial precursors and midbrain-like dopaminergic neurons from human embryonic stem cells using the bone morphogenic protein antagonist noggin. *Stem Cells* 25:411–418.
10. Tropepe V, et al. (2001) Direct neural fate specification from embryonic stem cells: A primitive mammalian neural stem cell stage acquired through a default mechanism. *Neuron* 30:65–78.
11. Ying QL, Stavridis M, Griffiths D, Li M, Smith A (2003) Conversion of embryonic stem cells into neuroectodermal precursors in adherent monoculture. *Nat Biotechnol* 21: 183–186.
12. McDonald JW, et al. (1999) Transplanted embryonic stem cells survive, differentiate and promote recovery in injured rat spinal cord. *Nat Med* 5:1410–1412.
13. Brüstle O, et al. (1999) Embryonic stem cell-derived glial precursors: A source of myelinating transplants. *Science* 285:754–756.
14. Kim JH, et al. (2002) Dopamine neurons derived from embryonic stem cells function in an animal model of Parkinson's disease. *Nature* 418:50–56.
15. Sharp J, Keirstead HS (2007) Therapeutic applications of oligodendrocyte precursors derived from human embryonic stem cells. *Curr Opin Biotechnol* 18:434–440.
16. Keirstead HS, et al. (2005) Human embryonic stem cell-derived oligodendrocyte progenitor cell transplants remyelinate and restore locomotion after spinal cord injury. *J Neurosci* 25:4694–4705.
17. Hochedlinger K, Jaenisch R (2006) Nuclear reprogramming and pluripotency. *Nature* 441:1061–1067.
18. Takahashi K, Yamanaka S (2006) Induction of pluripotent stem cells from mouse embryonic and adult fibroblast cultures by defined factors. *Cell* 126:663–676.
19. Okita K, Ichisaka T, Yamanaka S (2007) Generation of germline-competent induced pluripotent stem cells. *Nature* 448:313–317.
20. Wernig M, et al. (2007) In vitro reprogramming of fibroblasts into a pluripotent ES-cell-like state. *Nature* 448:318–324.
21. Maherali N, et al. (2007) Directly reprogrammed fibroblasts show global epigenetic remodeling and widespread tissue contribution. *Cell Stem Cell* 1:55–70.
22. Nakagawa M, et al. (2008) Generation of induced pluripotent stem cells without Myc from mouse and human fibroblasts. *Nat Biotechnol* 26:101–106.
23. Wernig M, Meissner A, Cassady JP, Jaenisch R (2008) c-Myc is dispensable for direct reprogramming of mouse fibroblasts. *Cell Stem Cell* 2:10–12.
24. Hanna J, et al. (2007) Treatment of sickle cell anemia mouse model with iPS cells generated from autologous skin. *Science* 318:1920–1923.
25. Wernig M, et al. (2008) Neurons derived from reprogrammed fibroblasts functionally integrate into the fetal brain and improve symptoms of rats with Parkinson's disease. *Proc Natl Acad Sci USA* 105:5856–5861.
26. Yamanaka S (2007) Strategies and new developments in the generation of patient-specific pluripotent stem cells. *Cell Stem Cell* 1:39–49.
27. Miura K, et al. (2009) Variation in the safety of induced pluripotent stem cell lines. *Nat Biotechnol* 27:743–745.
28. Okada Y, et al. (2008) Spatiotemporal recapitulation of central nervous system development by murine embryonic stem cell-derived neural stem/progenitor cells. *Stem Cells* 26:3086–3098.
29. Okada Y, Shimazaki T, Sobue G, Okano H (2004) Retinoic-acid-concentration-dependent acquisition of neural cell identity during in vitro differentiation of mouse embryonic stem cells. *Dev Biol* 275:124–142.
30. Niwa H, Miyazaki J, Smith AG (2000) Quantitative expression of Oct-3/4 defines differentiation, dedifferentiation or self-renewal of ES cells. *Nat Genet* 24:372–376.
31. Kumagai G, et al. (2009) Roles of ES cell-derived gliogenic neural stem/progenitor cells in functional recovery after spinal cord injury. *PLoS ONE* 4:e7706.
32. Masuda H, et al. (2007) Noninvasive and real-time assessment of reconstructed functional human endometrium in NOD/SCID/gamma c(null) immunodeficient mice. *Proc Natl Acad Sci USA* 104:1925–1930.
33. Miyoshi H, Blömer U, Takahashi M, Gage FH, Verma IM (1998) Development of a self-inactivating lentivirus vector. *J Virol* 72:8150–8157.
34. Okada S, et al. (2005) In vivo imaging of engrafted neural stem cells: Its application in evaluating the optimal timing of transplantation for spinal cord injury. *FASEB J* 19: 1839–1841.
35. Inoue Y, et al. (1986) Alteration of the primary pattern of central myelin in a chimaeric environment—study of shiverer ↔ wild-type chimaeras. *Brain Res* 391:239–247.
36. Bregman BS, et al. (1993) Recovery of function after spinal cord injury: Mechanisms underlying transplant-mediated recovery of function differ after spinal cord injury in newborn and adult rats. *Exp Neurol* 123:3–16.
37. Nygren LG, Fuxe K, Jonsson G, Olson L (1974) Functional regeneration of 5-hydroxytryptamine nerve terminals in the rat spinal cord following 5, 6-dihydroxytryptamine induced degeneration. *Brain Res* 78:377–394.
38. Hofstetter CP, et al. (2002) Marrow stromal cells form guiding strands in the injured spinal cord and promote recovery. *Proc Natl Acad Sci USA* 99:2199–2204.
39. Widenfalk J, Lundströmer K, Jubran M, Brene S, Olson L (2001) Neurotrophic factors and receptors in the immature and adult spinal cord after mechanical injury or kainic acid. *J Neurosci* 21:3457–3475.
40. McTigue DM, Horner PJ, Stokes BT, Gage FH (1998) Neurotrophin-3 and brain-derived neurotrophic factor induce oligodendrocyte proliferation and myelination of regenerating axons in the contused adult rat spinal cord. *J Neurosci* 18:5354–5365.
41. Courtine G, et al. (2009) Transformation of nonfunctional spinal circuits into functional states after the loss of brain input. *Nat Neurosci* 12:1333–1342.
42. Lu P, Tuszynski MH (2008) Growth factors and combinatorial therapies for CNS regeneration. *Exp Neurol* 209:313–320.
43. Okita K, Nakagawa M, Hyenjong H, Ichisaka T, Yamanaka S (2008) Generation of mouse induced pluripotent stem cells without viral vectors. *Science* 322:949–953.
44. Zhou H, et al. (2009) Generation of induced pluripotent stem cells using recombinant proteins. *Cell Stem Cell* 4:381–384.
45. Ogawa Y, et al. (2002) Transplantation of in vitro-expanded fetal neural progenitor cells results in neurogenesis and functional recovery after spinal cord contusion injury in adult rats. *J Neurosci Res* 69:925–933.
46. Pearse DD, et al. (2004) cAMP and Schwann cells promote axonal growth and functional recovery after spinal cord injury. *Nat Med* 10:610–616.
47. Pearse DD, et al. (2007) Transplantation of Schwann cells and/or olfactory ensheathing glia into the contused spinal cord: Survival, migration, axon association, and functional recovery. *Glia* 55:976–1000.
48. Iwanami A, et al. (2005) Establishment of graded spinal cord injury model in a nonhuman primate: The common marmoset. *J Neurosci Res* 80:172–181.
49. Iwanami A, et al. (2005) Transplantation of human neural stem cells for spinal cord injury in primates. *J Neurosci Res* 80:182–190.
50. Basso DM, et al. (2006) Basso Mouse Scale for locomotion detects differences in recovery after spinal cord injury in five common mouse strains. *J Neurotrauma* 23:635–659.

Clinical chart review of spinal cord injured pain

Hironobu Uematsu[1], Masahiko Shibata[2], Youko Matsumura[1]
Youichi Matsuda[1], Gaku Sakaue[1]
Takaya Inoue[3], and Takashi Mashimo[1]

[1]Department of Anesthesiology and Intensive Care, Osaka University Graduate School of Medicine
[2]Department of Pain Medicine, Osaka University Graduate School of Medicine
[3]Department of Kampo Medicine, Osaka University Graduate School of Medicine

[Received 21 December 2009, Accepted 15 February 2010]

Abstract

Clinical chart review of 49 cases with spinal cord injured pain was performed. Retrospective data about the characteristics of patients, the level of injury, the completeness of injury and the etiology was collected. Of pathogenesis of spinal cord injury, degenerative disease was 25 subjects (51%), 12 was traumatic (24%), 4 was vascular (8%) and 4 was neoplastic disease (8%). Thirty two subjects have injured at the cervical level (65%), 13 at the thoracic level (27%) and 4 at the lumbosacral level (8%). At-level neuropathic pain was present in 19 subjects (39%), below-level neuropathic pain was present in 42 subjects (85%). Gabapentin was effective in 24 patients (41%), clonazepam was effective in 17 (30%) and tricyclic antidepressants was effective in 21 patients (38%). We analized relationship between the characteristics of SCI pain and the result of various evaluation; Visual Analogue Scale (VAS), Hospital Anxiety Depression Scale (HAD), Pain Disability Assessment Scale (PDAS) and McGill Pain Questionnaire (MPQ).

Key words: Spinal cord injured pain; Classification of pain; Neuropathic pain; Gabapentin

PAIN RESEARCH 25 (2010) 19-25

当院における脊髄障害性疼痛症例の検討

植松 弘進[1]／柴田 政彦[2]／松村 陽子[1]／松田 陽一[1]
阪上 学[1]／井上 隆弥[3]／真下 節[1]

[1]大阪大学大学院 医学系研究科 生体統御医学 麻酔・集中治療医学講座
[2]大阪大学大学院 医学系研究科 疼痛医学寄附講座
[3]大阪大学大学院 医学系研究科 漢方医学寄附講座

はじめに

脊髄の損傷は外傷，変性疾患，血管障害，腫瘍，医療行為などによって起こる。その多くの患者は一時的ないしは慢性的に痛みで苦しむ。脊髄障害性疼痛は神経障害性疼痛と侵害受容性疼痛に分類され，神経障害性疼痛はさらに，神経障害部位に限局したAt-levelの痛みと障害部位より尾側に起こるBelow-levelの痛みに分類される。侵害受容性疼痛には，筋骨格系の痛みと内臓痛とがある[1,2]。脊髄障害性疼痛は，症例ごとに病態が異なり，治療に対する反応性も異なるため，個別的で丁寧な診療が求められる。脊髄障害性疼痛はあらゆる治療に反応しないこともまれではない。患者は痛みを我慢するか，極めて確率の低い侵襲的な治療にわずかな望みをかけて挑戦し，結果的に失望するかのいずれかであるのが現状である[3]。歴史的に，障害部位よりも上位での神経破壊的なアプローチが試みられたが，多くの場合無効であった[4]。これらの経験から脊髄障害性疼痛は，障害部位における神経細胞の異常発火のみではなく，上位の中枢神経系の機能変化が関与していると考えられるに至った。脊髄障害性疼痛に対する薬物治療の臨床研究は少なく，そのほかの神経障害性疼痛で得られたエビデンスを流用し，三環系抗うつ薬，抗てんかん薬，麻薬性鎮痛薬などの使用が推奨されている[5]。今後，本邦においても脊髄障害性疼痛の現況把握として多施設研究や薬物治療の臨床研究が必要である。

本研究では，大阪大学医学部附属病院における過去5年間の脊髄障害性疼痛症例について遡及的に検討した。

Table 1 Characteristics of the study sample

	Characteristic	Value
Age (yr)		
	Mean	61
	Range	31 – 76
Gender, *n* (%)	Male	31 (63)
	Female	18 (36)
Level of injury, *n* (%)		
	Cervical	32 (65)
	Thoracic	13 (27)
	Lumbosacral	4 (8)
Completeness of injury, *n* (%)		
	Complete	7 (14)
	Imcomplete	34 (69)
	No paralysis	8 (16)
Etiology, *n* (%)		
	Degenerative	25 (51)
	Traumatic	12 (24)
	Vascular	4 (8)
	Neoplastic	4 (8)
	Other	4 (8)

方　法

2004年1月から2009年4月までの大阪大学医学部附属病院麻酔科外来を受診した初診患者1,315名のうち49名の脊髄障害性疼痛患者について検討した。診療録を取り寄せ，性別・年齢・障害の部位・麻痺の程度・脊髄障害の病因についてデータを抽出し検討した。診療録の記載内容から判断し痛みを，「At-level」「Below-level」「内臓痛」「その他」の4つに分類した[1,2]。また，当科では何らかの効果が認められない薬剤は継続投与しないという方針で診療方針を統一しており，「当科で処方開始し継続されている薬剤とカルテに効果ありと記載がある薬剤」を「効果のあった薬剤」と仮定し検討し

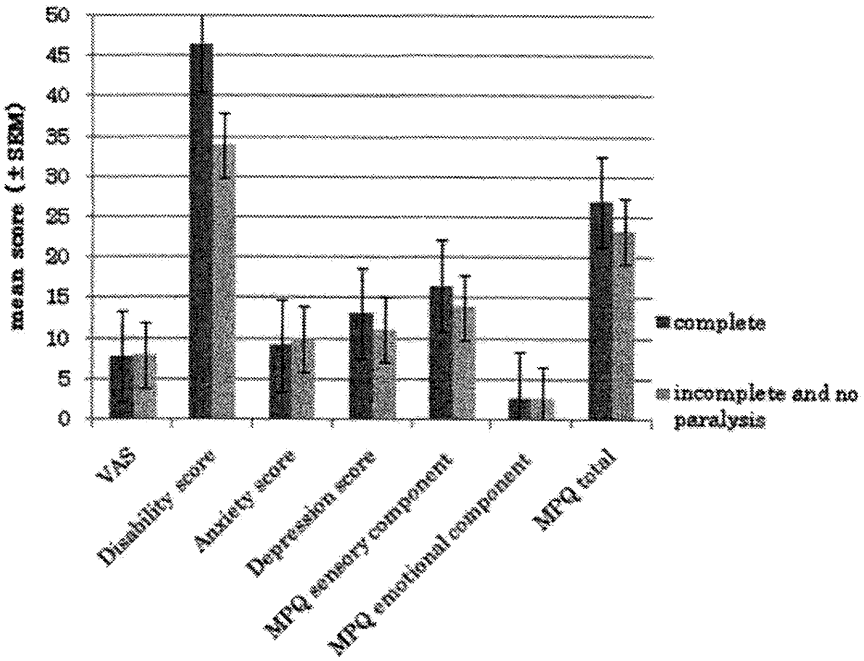

Fig.1 Pain, disability, anxiety, and depression score of SCI patients. There is no significant differences in pain, disability, anxiety and depression score between complete and incomplete paralytic patients.
VAS: Visual Analogue Scale, PDAS: Pain Disability Assessment Scale, HAD: Hospital Anxiety Depression Scale, MPQ: McGill Pain Questionnaire

た。当科では初診時に痛みの質的・量的評価として McGill Pain Questionnaire (MPQ) と Visual Analogue Scale (VAS) を，不安やうつなど情動的側面の評価として Hospital Anxiety Depression Scale (HAD) を，そして日常生活動作障害度の評価として Pain Disability Assessment Scale (PDAS) を使用しており，これらについても検討した。

結　果

年齢の平均は 61 歳 (31 歳から 76 歳) で 63% が男性であった (**Table 1**)。脊髄障害の部位は頸椎が 65%と最も多く，つづいて胸椎 (27%)，腰椎 (8%) であった。完全麻痺，不全麻痺はそれぞれ 14%，69%であった。病因で最も多かったのが変性疾患 (51%) であった。麻痺の様式によって HAD score で評価した不安・うつ，PDAS で評価した生活尺度，MPQ で評価した痛みの強さに差はなかった (**Fig.1**)。85%が Below-level の痛みを，39%が At-level の痛みを訴えており，24%が At-level と Below-level 両方の痛みを重複して訴えていた (**Fig.2-A**)。At-level の痛みもしくは Below-level の痛みのみを持つ患者に比べて，両方の痛みを持つ患者の方が MPQ の総合点が有意に高かった ($p<0.05$, Kruskal-Wallis test)。VAS で評価した痛みの強さ，HAD score で評価した不安・うつ，PDAS で評価した生活尺度に有意な差を認めなかった (**Fig.2-B**)。なんらかの効果のあった薬剤について **Fig.3** に示す。当院では脊髄障害性疼痛に対し他の神経障害性疼痛でエビデンスのある三環系抗うつ薬や抗てんかん薬のガバペンチン・クロナゼパムが最もよく使用され，一部の症例

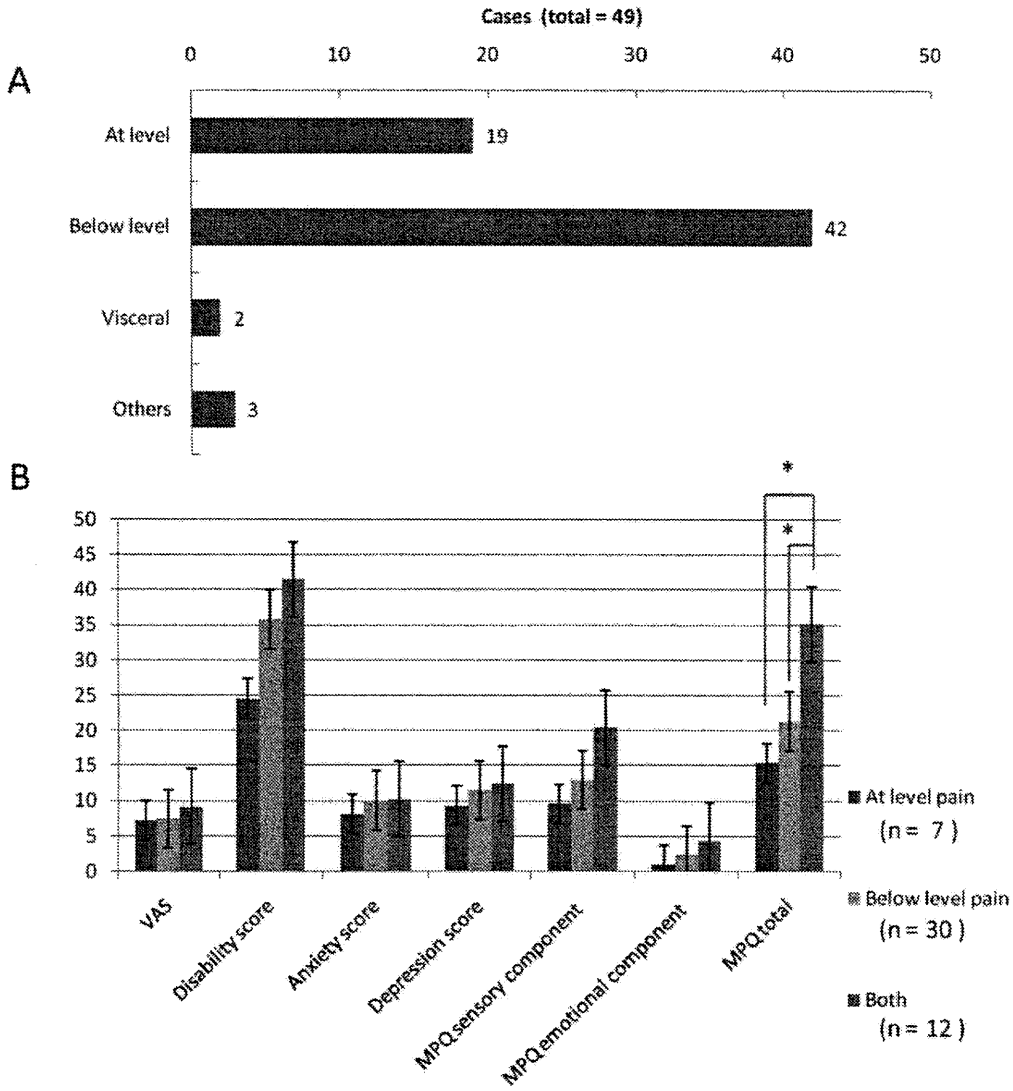

Fig.2 A: Classification of SCI pain. **B:** Pain, disability, anxiety, and depression score of SCI patients. There is no significant differences in pain, disability, anxiety and depression score between At-level pain, Below-level pain and both.
VAS: Visual Analogue Scale, PDAS: Pain Disability Assessment Scale, HAD: Hospital Anxiety Depression Scale, MPQ: McGill Pain Questionnaire, *p<0.05 Kruskal–Wallis test

で麻薬性鎮痛薬が処方されている[5]。当院で最もよく使用される三環系抗うつ薬，ガバペンチンとクロナゼパムについて治療前の VAS・MPQ・HAD・PDAS を比較したが一定の傾向は認められなかった (**Fig.4**)。

考　察

脊髄障害後の有痛者の割合は 5〜70%[6,7] から 81%[8] と報告により差が大きい。これは国や地域による脊髄障害の原因の違いや，データ収集の違いに起因すると考えられる[6]。本邦においては，2004 年に日本せきずい基金による「脊髄

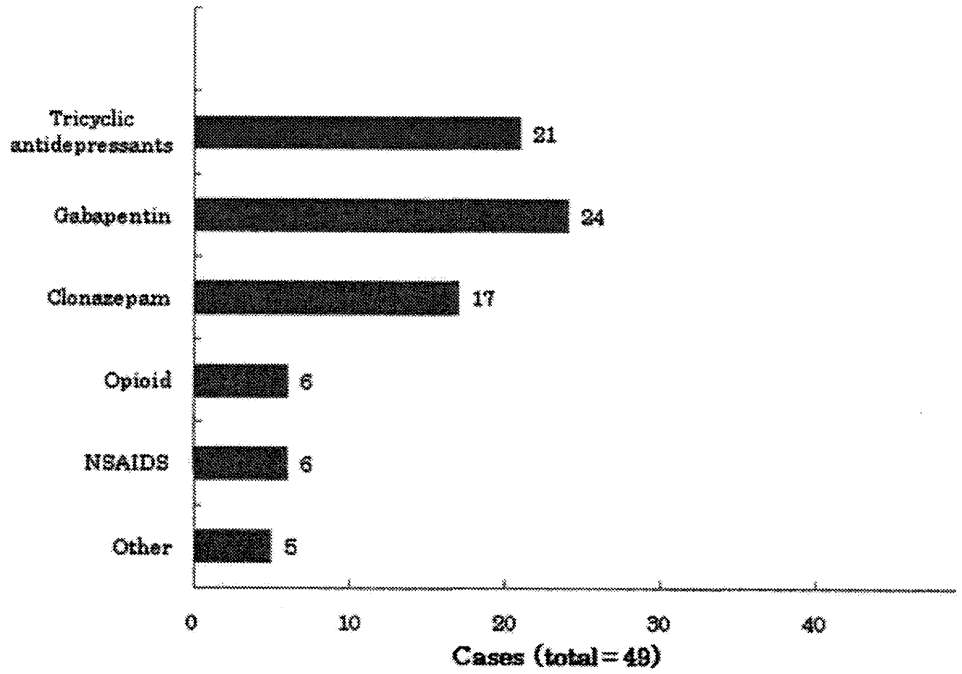

Fig.3 Effective drugs for SCI patients.

損傷に伴う異常疼痛」に関する実態調査報告書が発表され[3]，わが国における脊髄障害性疼痛に対する取り組みの遅れが指摘されている。このレポートは全国の在宅脊髄損傷者1,659名に対し行われたアンケート調査で，それによると全体の約75%に何らかの痛みがあるのにもかかわらず，痛みに対する治療がほとんど試みられておらず消炎鎮痛薬とビタミン剤のみ投与されているケースと，効果の可能性の低い神経破壊的治療法を実施され結果的に効果がなく心理的経済的に大きな負担となったケースと二極化しているのが現況である[3]。

過去の報告では，痛みの分類で筋骨格系の痛みが59%と最も多く，次いで神経障害性のAt-levelの痛みが41%，Below-levelの痛みが34%とされている[8]。本研究ではBelow-levelの痛みが85%とほとんどで，次いでAt-levelの痛みが39%であった。この違いは，本研究の対象患者の47%が頸椎症性頸髄症に対する後方除圧後に痛みが強く整形外科からペインクリニックへ紹介受診されてきた患者であったことが原因と考える。また，今回の結果では麻痺の程度や痛みの部位と強さ，日常生活動作に有意差は認められなかった。これらは脊髄障害性疼痛が症例毎に病態が大きく異なるためであると考える。

臨床研究によってプレガバリン，ガバペンチン，アミトリプチンは脊髄障害性疼痛に有効であるとされている[9,10,11]。本研究でも最も処方されている薬剤はガバペンチン，三環系抗うつ薬であった。また，脊髄損傷後疼痛患者においては抑うつ傾向のある患者においてアミトリプチンが有効であるという報告もあるが[11]，我々の結果では三環系抗うつ薬の反応性と治療前のうつ・不安スコアーとに関連性は認められなかった。本研究は統計解析するには症例数が限られており，今後は多施設大規模研究が必要である。

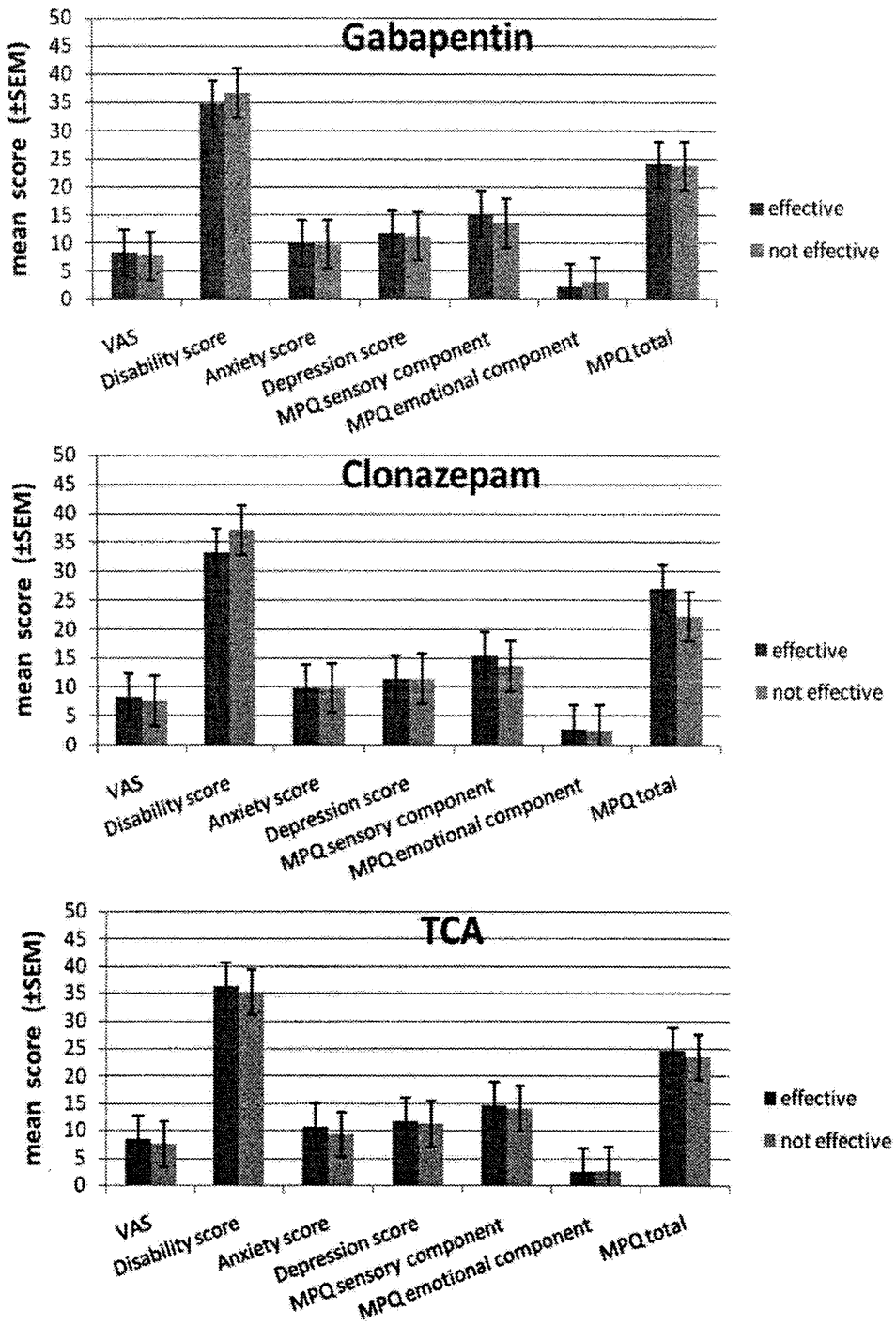

Fig.4 Pain, disability, and depression score of SCI patients There is no siginificant differences in pain, disability, anxiety and depression score between Gabapentin, Clonazepam and Tricyclic antidepressants.

結　論

脊髄障害性疼痛は治療反応性の乏しく，医学的に効果のある治療法も少ない。当院における脊髄障害性疼痛の実態としては，頸椎症性頸髄症を原因とする不全麻痺症例が47%と多かった。また，麻痺の重症度や痛みの分類など一定の傾向はみられず個々の症例で異なること，治療前の情動的要因や痛みの質的・量的相違にかかわらず薬物療法の治療効果はけっして高くはないことが明らかになった。したがって詳細な問診のうえ痛みの評価を行い，個々の症例毎に慎重に対応する必要がある。

脊髄障害性疼痛に関する研究は非常に少なく，本邦においてはその実態すら把握できていないのが現況である。今後早急に，多施設大規模研究が望まれる。

文　献

1) Siddall, P.J., Middleton, J.W., A proposed algorithm for the management of pain following spinal cord injury, Spinal Cord, 44 (2006) 67-77.
2) Siddall, P.J., Taylor, D.A., Cousins, M.J., Classification of pain following spinal cord injury, Spinal Cord, 35 (1997) 69-75.
3) 日本せきずい基金：脊髄損傷に伴う異常疼痛に関する実態調査報告書: SSK 日本せきずい基金レポート 07, 2004.
4) Melzack, R., Loeser, J.D., Phantom body pain in paraplegics: evidence for a central "pattern generating mechanism" for pain, Pain 4 (1978) 195-210.
5) Dworkin, R.H., O'Connor, A.B., Backonja, M., et al., Pharmacologic management of neuropathic pain: evidence-based recommendations, Pain, 132 (2007) 237-251.
6) Bonica, J.J., Introduction: semantic, epidemiologic, and educational issues. In: Casey KL, editor. Pain and central nervous system disease: the central pain syndromes, New York, NY: Raven Press, 1991, pp.13-29.
7) Ravenscroft, A.J., Chronic pain after spinal cord injury: a survey of practice in spinal injury units in the USA, Spinal Cord, 38 (2000) 658-660.
8) Siddall, P.J., McClelland, J.M., Rutkowski, S.B., et al., A longitudinal study of the prevalence and characteristics of pain in the first 5 years following spinal cord injury, Pain, 103 (2003) 249-257.
9) Tzellos, T.G., Papazisis, G., Amaniti, E., et al., Efficacy of pregabalin and gabapentin for neuropathic pain in spinal-cord injury: an evidence-based evaluation of the literature, Eur. J. Clin. Pharmacol., 64 (2008) 851-858.
10) Siddall, P.J., Cousins, M.J., Otte, A., et al., Pregabalin in central neuropathic pain associated with spinal cord injury: a placebo-controlled trial, Neurology, 67 (2006) 1792-1800.
11) Rintala, D.H., Holmes, S.A., Courtade, D., et al., Comparison of the effectiveness of amitriptyline and gabapentin on chronic neuropathic pain in persons with spinal cord injury, Arch. Phys. Med. Rehabil., 88 (2007) 1547-1560.

Address for correspondence: Hironobu Uematsu
Department of Anesthesiology and Intensive Care,
Osaka University Graduate School of Medicine
2-2 Yamadaoka, Suita, Osaka 565-0871, Japan
TEL: 06-6879-3745 / FAX: 06-6879-3495

Neuroscience 169 (2010) 994–1006

LAMINAE-SPECIFIC DISTRIBUTION OF ALPHA-SUBUNITS OF VOLTAGE-GATED SODIUM CHANNELS IN THE ADULT RAT SPINAL CORD

T. FUKUOKA,* K. KOBAYASHI AND K. NOGUCHI

Department of Anatomy and Neuroscience, Hyogo College of Medicine, 1-1 Mukogawa-cho, Nishinomiya, Hyogo, 663-8501, Japan

Abstract—While the voltage-gated sodium channels (VGSCs) are the key molecules for neuronal activities, the precise distribution of them in spinal cord is not clear in previous studies. We examined the expression of mRNAs for α-subunits of VGSC (Navs) in adult rat spinal cord before and 7 days after L5 spinal nerve ligation (SPNL) or complete Freund's adjuvant (CFA)-induced paw inflammation by *in situ* hybridization histochemistry, reverse transcription-polymerase chain reaction, and immunohistochemistry. Nav1.1 and Nav1.6 mRNAs were present in all laminae, except for lamina II, including the spinothalamic tract neurons in lamina I identified by retrograde tracing of Fluoro-gold. Nav1.2 mRNA was predominantly observed in the superficial layers (laminae I, II), and Nav1.3 mRNA was more restricted to these layers. All these transcripts were expressed by the neurons characterized by immunostaining for neuron-specific nuclear protein. Nav1.7 mRNA was selectively expressed by a half of motoneurons in lamina IX. No signals for Nav1.8 or Nav1.9 mRNAs were detected. Immunohistochemistry for Nav1.1, Nav1.2, Nav1.6, and Nav1.7 proteins verified some of these neuronal distributions. L5 SPNL decreased Nav1.1 and Nav1.6 mRNAs, and increased Nav1.3 and Nav1.7 mRNAs in the axotomized spinal motoneurons, without any changes in other laminae of L4–6 spinal segments. Intradermal injection of CFA did not cause any transcriptional change. Our findings demonstrate that spinal neurons have different compositions of VGSCs according to their location in laminae. Pathophysiological changes of spinal neuronal activity may due to post-transcriptional changes of VGSCs. Comparison with our previous data concerning the subpopulation-specific distribution of Nav transcripts in primary afferent neurons provides potentially specific targets for local analgesics at the peripheral nerve and spinal levels.

Key words: Nav, neuropathic pain, complete Freund's adjuvant.

The spinal gray matter is classified into 10 different laminae containing morphologically and functionally different neurons (Rexed, 1952). Among them, laminae I–V are mainly involved in sensory processing. Lamina II neurons are especially important, receiving modulatory input from supraspinal regions. Lamina I contains projection neurons to some upper brain regions. On the other hand, spinal motoneurons innervating all skeletal muscles of the extremities and body trunk are located in lamina IX.

Voltage-gated sodium channels (VGSCs) are key molecules involved in action potential generation and propagation of all neurons throughout the nervous system. The main component of these channels is the α-subunits including the pore-forming loop, the voltage sensor, and a Na^+ selective filter. To date, nine different α-subunits (Navs) have been cloned and named Nav1.1–1.9 (Goldin et al., 2000). Although these Navs appear to be differently expressed throughout the nervous system and their distribution has been widely examined, our knowledge about the precise distribution of these Navs in spinal cord is limited (Felts et al., 1997; Toledo-Aral et al., 1997; Krzemien et al., 2000; Tzoumaka et al., 2000; Lindia and Abbadie, 2003).

Recently, using high sensitive riboprobes for Nav1.1–1.3, and Nav1.6–1.9 mRNAs, we have revealed a more precise description of the distribution of these transcripts among the histochemically-identified neuronal subpopulations of adult rat dorsal root ganglion (DRG) than in previous studies (Black et al., 1996; Sangameswaran et al., 1996; Felts et al., 1997; Toledo-Aral et al., 1997; Dib-Hajj et al., 1998; Novakovic et al., 1998; Fukuoka et al., 2008). The first purpose of this study was to examine, in detail, the exact localization of Nav1.1–1.3, and Nav1.6–1.9 mRNAs and proteins in the naive adult rat spinal cord. The second purpose was to reveal the transcriptional changes of these Navs in pathological states, especially in relation to L5 spinal nerve ligation (SPNL) and peripheral inflammation induced by intradermal injection of complete Freund's adjuvant (CFA).

EXPERIMENTAL PROCEDURES

Animals

Male Sprague–Dawley rats (Nippon Dobutsu Co., Nishinomiya, Japan; 230–280 g) were housed in plastic cages, 3–4 per cage, and food and water were available *ad libitum*. The room was maintained on a 12-h light/dark cycle in a constant 22–24 °C temperature. All surgical procedures and drug injections were done on rats that were deeply anesthetized with sodium pentobarbital (50 mg/kg and additional doses as needed, i.p., Kyoritsu Seiyaku Co., Tokyo, Japan). All animal experimental procedures conformed to the regulations of the Hyogo College of Medicine Committee on Animal Research and adhered to the National

*Corresponding author. Tel: +81-798-45-6416; fax: +81-798-45-6417.
E-mail address: tfukuoka@hyo-med.ac.jp (T. Fukuoka).

Abbreviations: CCI, chronic constriction injury; CFA, complete Freund's adjuvant; DRG, dorsal root ganglion; FG, fluoro-gold; IHC, immunohistochemistry; ISHH, *in situ* hybridization histochemistry; NeuN, neuron-specific nuclear protein; NHS, normal horse serum; RT-PCR, reverse transcription-polymelase chain reaction; SPNL, spinal nerve ligation; TBS, Tris-buffered saline; VGSC, voltage-gated sodium channels.

0306-4522/10 $ - see front matter
doi:10.1016/j.neuroscience.2010.05.058

Institute of Health Guide for the Care and Use of Laboratory Animals. All efforts were made to minimize the number of animals used and their suffering.

Surgical procedures and behavioral tests

Four rats received a unilateral L5 SPNL, as described previously (Kim and Chung, 1992; Fukuoka et al., 2008). Another four rats received an intradermal injection of 100 μl CFA (Calbiochem, La Jolla, CA, USA) into the plantar surface of the left hind paw. Tests of thermal and mechanical withdrawal thresholds of plantar surface of the bilateral hind paws were done in all rats just before, and 1, 3, and 7 days after surgery or injection. The withdrawal latency of the hind paw to a radiant heat was automatically measured using the plantar test (model 7370, Ugo Basile, Comerio, Italy). The three latencies per side were averaged to obtain the withdrawal latency. Mechanical withdrawal threshold was assessed with a dynamic plantar aesthesiometer (model 37450, Ugo Basile). The mean value of three trials with at least 5 min intervals between trials was taken as the withdrawal threshold. Data were expressed as mean±SEM. Differences in the values over time were tested using one-way repeated measures ANOVA followed by Fisher's protected least significant difference test. Two-tailed *P*-values less than 0.05 were considered to be significant. After the final behavioral measurement, all rats were deeply anesthetized with pentobarbital (75 mg/kg i.p.) and processed for tissue preparation as described below.

Retrograde tracing of spinal neurons projecting to the thalamus

Three rats were anesthetized with pentobarbital (50 mg/kg i.p.) and received an injection of Fluoro-gold (FG; Fluorochrome Inc., Englewood, UK) into the brain. Briefly, the skull was fixed into a stereotaxic frame (Narishige, Tokyo, Japan). Each rat received a pressure injection of 100–200 nl 4% FG through a glass micropipette attached to the needle of a 10 μl Hamilton microsyringe into the thalamus on the right side. Injections were centered in the ventrolateral thalamic nucleus according to the atlas of Paxinos and Watson (1986) (2 mm caudal from Bregma, 2 mm lateral, and 6.2 mm of depth) because injections around this region label spinothalamic tract neurons in the rat (Burstein et al., 1990). Seven days after injection, the rats were deeply anesthetized with pentobarbital (75 mg/kg i.p.) and processed for tissue preparation as described below.

Tissue preparation

At the fixed time, the rats were sacrificed by decapitation under deep anesthesia. The lumbar (L4–6) and cervical (C5–6 for FG study only) spinal cord segments were quickly dissected out, rapidly frozen in powdered dry ice, cut on a cryostat at a 16 μm thickness, and thaw-mounted onto Mas-coated glass slides (Matsunami, Osaka, Japan). We used three other rats as naive control without any of the above-mentioned surgeries or injections. With regard to the sections obtained from the rats that received FG injections, we took photographs of the sections containing FG-labeled neurons before *in situ* hybridization histochemistry (*in situ* hybridization histochemistry (ISHH)) through an OLYMPUS BX50 microscope under incident UV light with a 330–385 nm band pass filter. The adequate fields were digitized with the connected Nikon DXM-1200 digital camera, captured, and saved as TIFF files using ACT-1 software (Nikon, Tokyo, Japan).

Reverse transcription (RT)-polymerase chain reaction (PCR) and ISHH

Total RNA was extracted from adult rat spinal cord. Reverse transcription-polymelase chain reaction (RT-PCR) and ISHH using the α^{35}S-UTP-labeled cRNA probes for Nav1.1–1.3 and Nav1.6–1.9 were carried out as described previously (Fukuoka et al., 2008).

Immunohistochemistry (IHC) for Navs

Three naive rats were deeply anesthetized with pentobarbital (100 mg/kg i.p.) and perfused through the ascending aorta with freshly prepared 4% formaldehyde in 0.1 M PB. The L4–5 spinal cords were removed, postfixed in the same fixative for 4–5 h, and then cryoprotected in 20% sucrose in 0.1 M PB at 4 °C overnight. Twenty-five micrometres free-floating transverse sections were cut on a cryostat and collected into Tris-buffered saline (TBS). These spinal cord sections were immunostained using the following rabbit polyclonal antibodies at the indicated dilution: Nav1.1 (1:300, ASC-001), Nav1.2 (1:3000, ASC-002), Nav1.6 (1:1000, ASC-009), and Nav1.7 (1:1000, ASC-008, all purchased from Alomone Laboratories, Jerusalem, Israel). Western blot data of rat brain membranes using these antibodies are provided in the data sheets. All immunohistochemical staining of spinal cord (Fig. 5) was abolished when the diluted primary antibodies were preincubated with the same weight of the epitope peptides provided from the manufacture (data not shown). These antibodies have been used for immunohistochemistry of rat tissue sections in previous studies except for the anti-Nav1.2 antibody (Black et al., 2004; Wittmack et al., 2004). The anti-Nav1.2 antibody, however, has been well characterized by immunoblot of Nav1.2 knockout mice brain membranes (Planells-Cases et al., 2000). The detail immunohistochemical procedure was described previously (Fukuoka et al., 2001).

IHC combined with ISHH

In order to distinguish the neurons from other cells, we used a monoclonal antibody (MAB377, Chemicon, Temecula, CA, USA) for neuron-specific nuclear protein (NeuN). The cryostat sections were fixed in 4% formaldehyde in 0.1 M PB for 20 min. After washing in 0.1 M Tris-buffered saline (TBS) three times each for 5 min, these sections were pre-incubated in TBS containing 10% normal horse serum (NHS) for 30 min, followed by incubation in the first antibody (1:1000) in TBS containing 5% NHS for 15 min at room temperature. The sections were washed in TBS and then incubated in biotinylated anti-mouse IgG (1:200; Vector Laboratories, Burlingame, CA, USA) in phosphate-buffered saline containing 5% NHS and 100 U/ml RNase inhibitor for 1 h at room temperature, followed by incubation in 30% methanol and 1% hydrogen peroxidase in TBS for 15 min to inactivate endogenous peroxidase. Then, the sections were incubated in avidin-biotin-peroxidase complex (Elite ABC kit; Vector) for 30 min at room temperature. The horseradish peroxidase reaction was developed for 4–5 min in TBS containing 0.05% 3,3′-diaminobenzidine tetrahydrochloride (Wako, Tokyo, Japan) and 0.01% hydrogen peroxidase. After three washes in TBS, sections were immediately processed for ISHH.

Image analysis

In order to objectively evaluate the change in expression of Nav mRNA in the L5 spinal motoneurons following L5 SPNL, we analyzed the density of silver grains over all neuronal profiles with obviously large cell bodies in the ventral horns of the randomly selected L5 sections using a computerized image analysis system (NIH Image, version 1.61). At a magnification of 200× and with bright-field illumination, upper and lower thresholds of gray level density were set such that only silver grains were accurately discriminated in the picture, and the percentage of the grain-occupied area in the each outlined neuronal profile was calculated by the computer. In the same manner, four background areas between motoneurons in the same ventral horn were randomly

established for each picture. The mean percentage of the four background areas was taken as the background grain density of the picture. To reduce the risk of biased sampling of the data owing to varying emulsion thickness, the percentage of grain-occupied area of each neuronal profile was divided by the background grain density giving a signal/noise (S/N) ratio. The S/N ratio of an individual neuron was plotted and compared between ipsilateral and contralateral side to L5 SPNL. At least 50 profiles from four rats were evaluated for each side and each transcript. We used Wilcoxon Signed Rank test for statistical analysis.

Photomicrographs

The representative pictures were digitized with a Nikon DIAPHOT-300 microscope connected to a Nikon DXM-1200 digital camera with darkfield or brightfield illumination. We used Adobe Photoshop 6.0 (Adobe Systems, Mountain View, CA, USA) to adjust the brightness and contrast of the images and to make all figures. In order to make Fig. 4, we compared the ISHH sections with the before-saved TIFF images and identified the spinothalamic neurons in the ISHH sections using at least two landmarks in the tissue and the image, such as other conspicuous cells.

RESULTS

Nav transcripts in the naive spinal cord

Dark-field photomicrographs of the transverse sections of spinal cord processed for ISHH clearly revealed unique distributions of Nav1.1–1.7 transcripts in laminae-specific manners (Fig. 1).

Nav1.1 and Nav1.6. The distributions of Nav1.1 and 1.6 transcripts were very similar (Fig. 1A, D). These signals were seen throughout the gray matter including the spinal motoneurons in ventral horn. Lamina II was, however, clearly seen as a band with lower signals for these mRNAs. At higher-magnifications, this tendency was verified (Fig. 2A, D). This was especially the case for signals of Nav1.6 mRNA. The signals were almost completely absent in the inner part of lamina II (Fig. 2D). On the other hand, some lamina I cells were strongly labeled for these mRNAs (arrowheads in Fig. 2A, D). In addition, many large-sized cells with high signals were present mainly in lamina IV.

Nav1.2 and Nav1.3. ISHH for Nav1.2 mRNA showed relatively even labeling throughout the gray matter with somewhat heavier labeling over the dorsal horn as compared to the ventral horn, with a tendency to concentrate in the superficial layers (Figs. 1B and 2B). Signals for Nav1.3 mRNA were mainly accumulated in the superficial layers, while some positive signals were observed in deeper layers, too (Figs. 1C and 2C). In contrast to Nav1.1 and 1.6, lamina II contained strong signals for Nav1.2 and Nav1.3 mRNAs, and the large-sized cells in lamina IV were not labeled for these mRNAs (Fig. 2B, C). The silver grains for Nav1.2 and 1.3 transcripts were concentrated over the nuclei of naive spinal motoneurons (see the contralateral side of L5 SPNL in Fig. 8B, C). Therefore, these signals appeared like small cells in ventral horn with darkfield illumination (Fig. 1B, C). A similar intracellular distribution has also been observed in naive DRG neurons (Fukuoka et al., 2008). Anyway, expression of these mRNAs in naive spinal motoneurons was very low.

Nav1.7. A limited number of spinal motoneurons (Fig. 1E, arrowhead in Fig. 8E) were moderately labeled for Nav1.7 mRNA, while other motoneurons completely lacked this transcript (Fig. 8E, O). No signals were detected in other parts of the naive spinal cord.

Nav1.8 and Nav1.9. There was no signal for these transcripts in any part of the naive spinal cord (Fig. 1F, G). RT-PCR clearly revealed the presence of Nav1.1–Nav1.7 transcripts, and the absence of Nav1.8 and Nav1.9 mRNAs in spinal cord (Fig. 1H).

Spinal neurons express multiple Nav mRNAs

In order to characterize the cells expressing Nav mRNAs in spinal cord, we used ISHH combined with IHC for NeuN (Fig. 3). NeuN-immunoreactive (ir) neurons, but not other cells stained in light purple by hematoxylin, expressed Nav1.1, Nav1.2, Nav1.3, and Nav1.6 transcripts. Signals for Nav1.1 and Nav1.6 mRNAs were accumulated over some neurons in lamina I (arrows in Fig. 3A, G), but not those in lamina II (seen in the lower part of each panel). Many, but not all, neurons in laminae III and IV also expressed these mRNAs (Fig. 3B, H). Signals for Nav1.2 and Nav1.3 mRNAs were detected in lamina II (Fig. 3C, E). In deeper layers of the dorsal horn, however, Nav1.3 mRNA was not detected (Fig. 3F), while Nav1.2 signals were seen in some lamina III neurons (arrowhead in Fig. 3D). The lack of Nav1.3 signals in the deeper layers may due to the facts that these signals are relatively weak and ISHH loses its high sensitivity after IHC procedure.

Spinothalamic tract neurons express Nav1.1 and Nav1.6 mRNAs

We found ISHH signals for Nav1.1 and Nav1.6 in lamina I (Figs. 2 and 3). This layer contains projection neurons whose axons ascend through the spinal cord and end in some brain regions, including thalamus (Kobayashi, 1998). Thus, we injected FG into the thalamus to retrogradely label spinal projection neurons, and then examined the expression of these two transcripts. As reported previously (Kobayashi, 1998; Al-Khater et al., 2008), much many spinal projection neurons were labeled in cervical dorsal horn (1.7 neurons/section in C5–6) than the lumbar segment (~0.2 neurons/section in L4–6). Of the identified cervical projection neurons, 100% (22/22) and 92% (24/26) were labeled for Nav1.1 and Nav1.6 mRNAs, respectively. At the lumbar segments, all (8/8 each) identified projection neurons were labeled for these transcripts. Fig. 4 represents examples of the latter.

Immunohistochemical staining of Navs in spinal cord

In order to verify the neuronal expression of Nav proteins, we explored immunohistochemistry of the naive rat spinal cord (Fig. 5). At low power view, the overall gray matter was lightly immunostained for Nav1.1, Nav1.2, and Nav1.6 (Fig. 5A, D, G). At higher power view, however, several densely stained components were observed. Anti-Nav1.1 antibody intensely labeled motoneurons in the spinal ventral horn (Fig. 5A), large cells in lamina I (arrows in Fig.

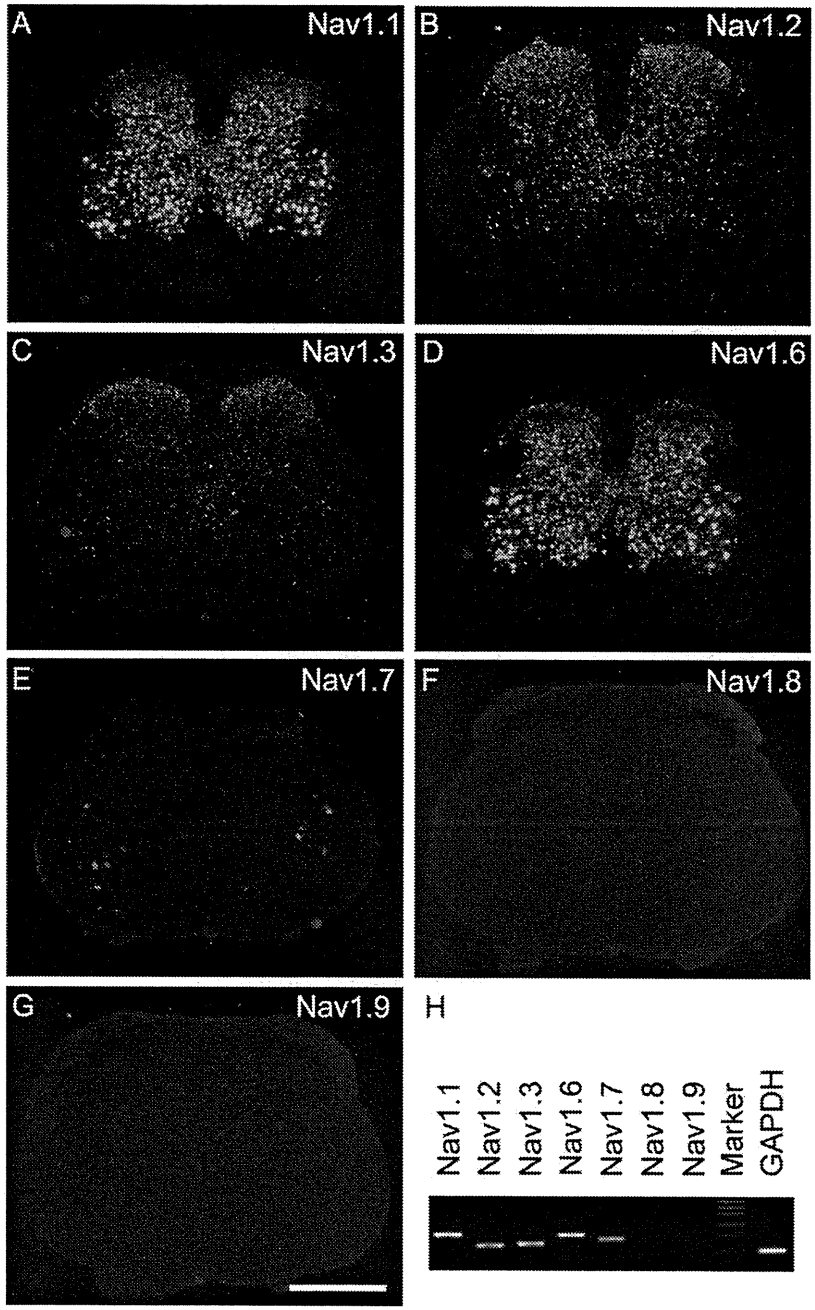

Fig. 1. (A–G) Darkfield photomicrographs of a transverse section of naïve rat L5 lumbar spinal cord showing *in situ* hybridization signals for Nav1.1, Nav1.2, Nav1.3, Nav1.6, Nav1.7, Nav1.8, and Nav1.9 mRNAs, respectively. The upper side of each panel is the dorsal side of the spinal cord. Note the laminae-specific distributions of Nav1.1–1.7 mRNAs. There were no signals for Nav1.8 or Nav1.9 in any part of spinal cord. Scale bar, 1 mm. (H) Expression of Nav mRNAs in naïve spinal cord by RT-PCR. Nav1.1–Nav1.7 transcripts were detected near the expected sizes (Nav1.1, 541 base; Nav1.2, 371 base; Nav1.3, 395 base; Nav1.6, 510 base; Nav1.7, 442 base), while Nav1.8 and Nav1.9 were not detected. GAPDH, positive control.

5B), and many cells in deeper layers (Fig. 5C). In addition, some small cells in the outer part of lamina II were also moderately labeled (arrowheads in Fig. 5B). For Nav1.2, many short varicose fibers were intensely, and some neuron-like profiles were moderately stained in the dorsal horn (arrowheads in Fig. 5E). In the deeper layers, many intensely labeled long varicose fibers were observed, while almost no immunopositive cells were identified (Fig. 5F). A limited number of spinal motoneurons were just detectable in the ventral horn (arrowheads in Fig. 5D). The background staining was denser in the superficial dorsal horn as compared to the deeper layers (Fig. 5E, F). Nav1.6-immunoreactivity was found in many spinal motoneurons (Fig. 5G), some neurons in lamina I or the outer part of lamina II (arrows in Fig. 5H), and many neurons in the deeper laminae (arrowheads in Fig. 5I). Nav1.7-immunoreactivity was largely restricted to the superficial layers of the dorsal horn (Fig. 5J). Close observation revealed many

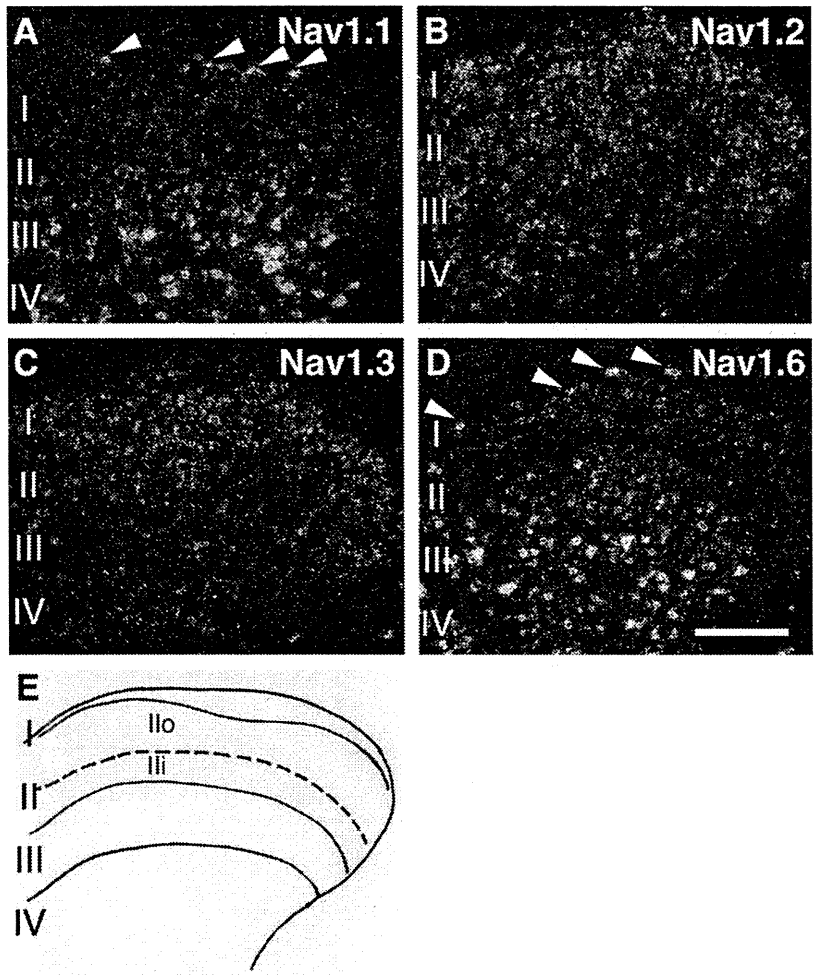

Fig. 2. High-magnification images showing the laminae-specific distribution of Nav1.1 (A), Nav1.2 (B), Nav1.3 (C), and Nav1.6 (D) mRNAs in naïve dorsal horn. A representative drawing of the borderlines between laminae is shown in panel (E). IIo and IIi, outer and inner parts of lamina II, respectively. Note the strong signals for Nav1.1 and Nav1.6 mRNAs in lamina I (arrowheads in A, D), and those in deeper layers (laminae III and IV). In contrast, signaling was very low in lamina II. Signals for Nav1.2 mRNA were seen all layers, while those for Nav1.3 were mostly restricted to the superficial layers of dorsal horn. Scale bar, 200 μm.

intensely stained fibers were distributed these layers (Fig. 5K). Although spinal motoneurons had just detectable staining (arrowheads in Fig. 5L), no other cell profiles were identified in the gray matter.

Pain behavior

Both L5 SPNL and CFA injection induced significant changes of mechanical threshold and withdrawal latency on the ipsilateral side (Fig. 6). Significant decreases were observed within a few days and continued until 7 days after surgery. There was no significant change on the contralateral side ($P>0.05$).

Nav transcripts in spinal cord after L5 SPNL

We examined at least 30 L4–6 spinal sections pooled from four animals for each probe. Transcriptional changes of Nav mRNAs were restricted in the spinal motoneurons of the L5 segment 7 days after L5 SPNL (Fig. 7), when thermal hyperalgesia and mechanical allodynia were present. No significant changes were observed in other parts of the L5 spinal segment or any parts in other examined spinal segments (L4 and L6; data not shown).

Nav1.1 and Nav1.6 ISHH signals for these two mRNAs were slightly decreased in the directly axotomized spinal motoneurons (arrowheads in Fig. 7A, D). Brightfield view and quantitative evaluation demonstrated these changes were statistically significant (Fig. 8). The axotomized motoneurons, however, still had relatively high level of signals (median S/N ratio ~40).

Nav1.2. Change in Nav1.2 expression was small and barely observable (Figs. 7B and 8B, C), however, the level was increased slightly in the axotomized motoneurons ($P=0.037$; Fig. 8L).

Nav1.3 and Nav1.7 SPNL clearly increased the signals for these two mRNAs in the axotomized motoneurons (arrows in Fig. 7C, E). These changes were also obvious with brightfield illumination (Fig. 8C, E, H, J),

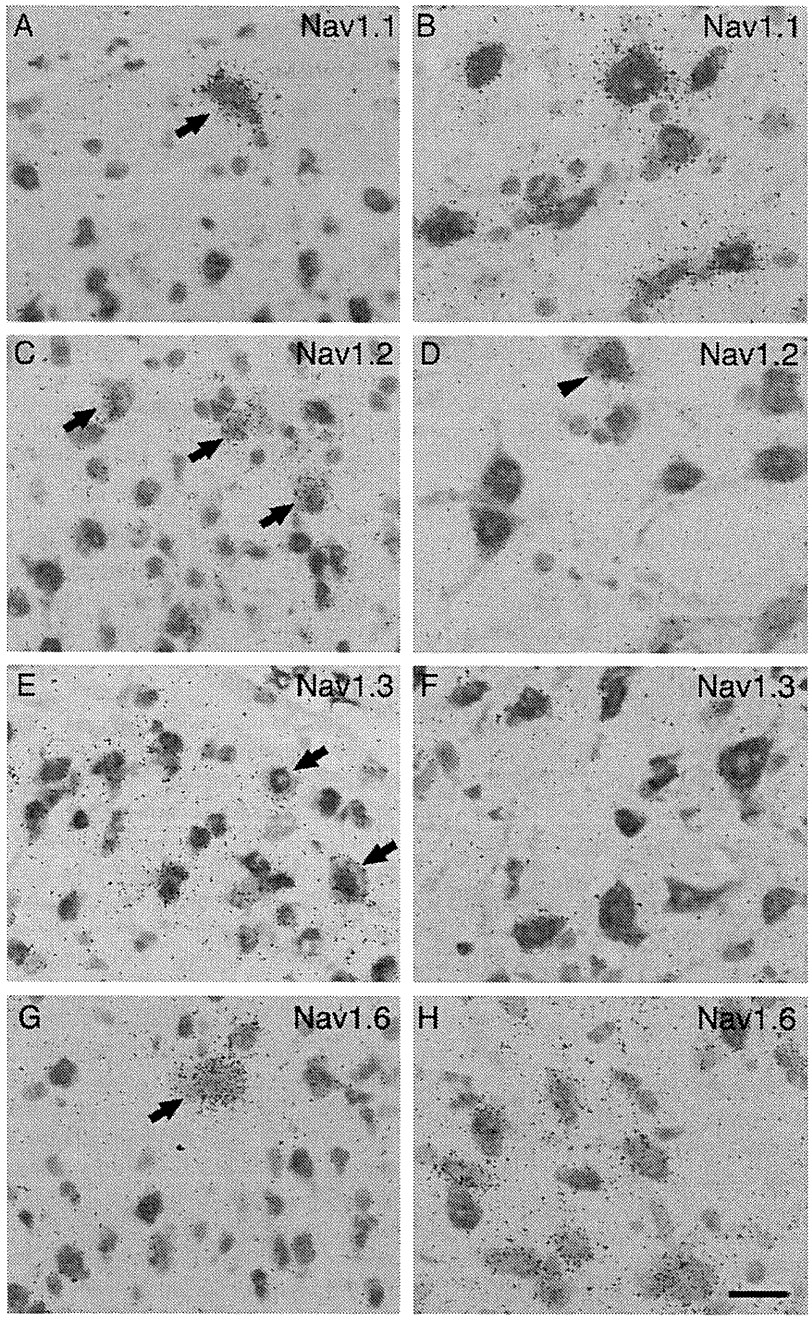

Fig. 3. Navs are expressed only by spinal neurons. Brightfield photomicrographs of superficial layers (laminae I and II, A, C, E, G) and deeper layers (laminae III and IV, B, D, F, H) of spinal dorsal horn sections treated with combined immunohistochemistry for the neuronal marker NeuN (brown) with ISHH for Nav1.1 (A, B), Nav1.2 (C, D), Nav1.3 (E, F), and Nav1.6 (G, H) mRNAs. The upper side of each panel is the dorsal side of spinal cord. Nuclei of glial cells are stained pale violet with Hematoxyline. Note that NeuN-ir neurons exclusively expressed these mRNAs. Arrows indicate examples of double-labeled lamina I neurons. Scale bar, 20 μm.

and image analysis confirmed that these changes were significant (Fig. 8M, O).

Nav transcripts after CFA induced inflammation

The expression of Nav mRNAs in the spinal cord 7 days after CFA injection, when thermal hyperalgesia and mechanical allodynia had developed, was qualitatively and quantitatively similar to that in the naive spinal cord (Fig. 1). No changes were observed for all examined Navs in any regions of the examined lumbar spinal segments (at least 28 L4–6 spinal sections pooled from four rats for each probe; data not shown).

DISCUSSION

Previous studies on Nav expression in the adult rat spinal cord have demonstrated that Nav1.1, Nav1.2 and Nav1.6

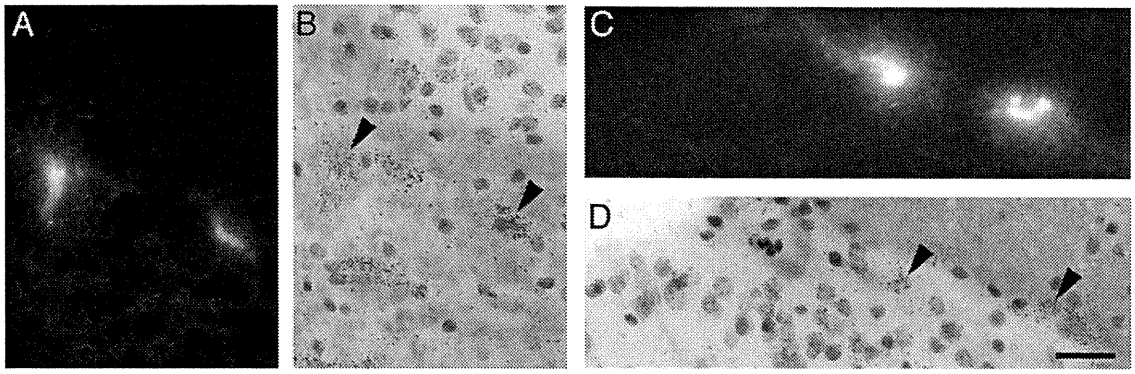

Fig. 4. Projection neurons express Nav1.1 and Nav1.6 transcripts. Microinjection of Fluorogold unilaterally into the thalamus retrogradely labeled a limited number of cells in the lateral spinal nucleus (A) and the marginal zone (C) in the L5 spinal segment. All these labeled neurons express Nav1.1 (B) and Nav1.6 mRNAs (D). Scale bar, 20 μm. For interpretation of the references to color in this figure legend, the reader is referred to the Web version of this article.

are present, Nav1.3 exhibits very low expression, and Nav1.7 is absent within the gray matter (Westenbroek et al., 1989; Felts et al., 1997; Krzemien et al., 2000; Tzoumaka et al., 2000; Lindia and Abbadie, 2003; Jarnot and Corbett, 2006). In this study, we confirmed some of these data, and extended them by detection of Nav1.3 and Nav1.7 mRNAs and by demonstrating laminae-specific neuronal distributions of these Navs.

Laminae-specific expression of Navs

The distributions of Nav1.1–1.3 and Nav1.6 mRNAs in the spinal dorsal horn were characteristic (Fig. 1). Given the higher level of signals for Nav1.1 and Nav1.6 mRNAs in the gray matter as compared to other Navs (Fig. 1A, D), it is clear that these two α-subunits are the main component of VGSCs in most of spinal neurons, except for in lamina II. One of the striking regions with high signals for Nav1.1 and Nav1.6 was lamina I (Figs. 2A, D and 5B, H). Neurons in this layer play important roles in nociception and many of them have ascending axons to brain regions that contribute to sensory processing, including the thalamus, parabrachial region, and medullary reticular formation (Menetrey et al., 1982; Burstein et al., 1990; Craig, 1995). We demonstrated that almost all (92–100%) spinothalamic tract neurons in lamina I intensely expressed Nav1.1 and Nav1.6 mRNAs (Fig. 4). Therefore, these two subunits seem to compose the main VGSCs that contribute action potential propagation for long distance through spinal cord. Other cells with noticeable Nav1.1 and Nav1.6 labeling were the large-sized cells in lamina IV (Fig. 2A, D). Since these cells were not labeled for Nav1.2, or Nav1.3 (Fig. 2B, C), they appear to possess only Nav1.1 and Nav1.6 as VGSCs. Although their identities are not clear in this study, given their large cell body in lamina IV, they may be "antenna cells," whose dendrites are so wide and long that they penetrate lamina II, and this type of neuron is thought to be a major output from lamina II (Willis and Coggeshall, 2004).

Neurons in the lamina II, especially the inner part of this layer, appear to have different compositions of VGSCs from those of other laminae neurons with low expression of Nav1.1 and Nav1.6 mRNAs. Given that lamina II neurons are interneurons having short axons and dendrites confined within the lamina (Willis and Coggeshall, 2004), they may not need a high level of Nav1.1 and Nav1.6. In compensation for this, Nav1.2 mRNA was relatively concentrated (Figs. 1B and 2B) and Nav1.3 mRNA was more restricted to this layer (Figs. 1C and 2C), suggesting that the native sodium currents recorded in this lamina are mainly composed of these two α-subunits. Since the lamina II neurons receive noxious input through the unmyelinated C and finely myelinated Aδ primary afferents and play important modulatory roles in nociceptive transmission, selective blockade of Nav1.3 may provide somewhat selective interruption of nociceptive transmission at the spinal level. Regarding nociceptive input, all neurofilament-negative primary afferents, presumably including nociceptors, express VGSCs composed of Nav1.7/1.8/1.9 and lack other Navs, including Nav1.2 and Nav1.3 (Fukuoka et al., 2008). Since Nav1.7, Nav1.8, and Nav1.9 are absent in any sensory processing laminae of dorsal horn (Fig. 1), the nociceptive input from C-fiber afferents should be relayed between membranes with completely different VGSCs at the first synapse in dorsal horn. Systemic or intrathecal application of selective blockers to Nav1.8 and Nav1.9 may exert a nociceptor-specific presynaptic conduction block with minimum effect on the spinal cord function (Jarvis et al., 2007).

We detected high signals for Nav1.1 and Nav1.6 mRNAs in spinal motoneurons (Fig. 8A, D). These observations are consistent with previous studies (Westenbroek et al., 1989; Schaller et al., 1995; Porter et al., 1996; Garcia et al., 1998; Lindia and Abbadie, 2003). In addition, we detected signals for Nav1.2 and Nav1.3 mRNAs in these neurons for the first time (Fig. 8B, C). Furthermore, we found that roughly 10–20% of motoneurons expressed Nav1.7 mRNA (Fig. 2E), which was not detected previously (Felts et al., 1997). Spinal motoneurons send their long axons through the ventral root and join the primary afferent fibers of DRG neurons in peripheral nerve. Since the main α-subunits in naive spinal motoneurons are Nav1.1 and Nav1.6 (Figs. 1 and 8), and nociceptor type

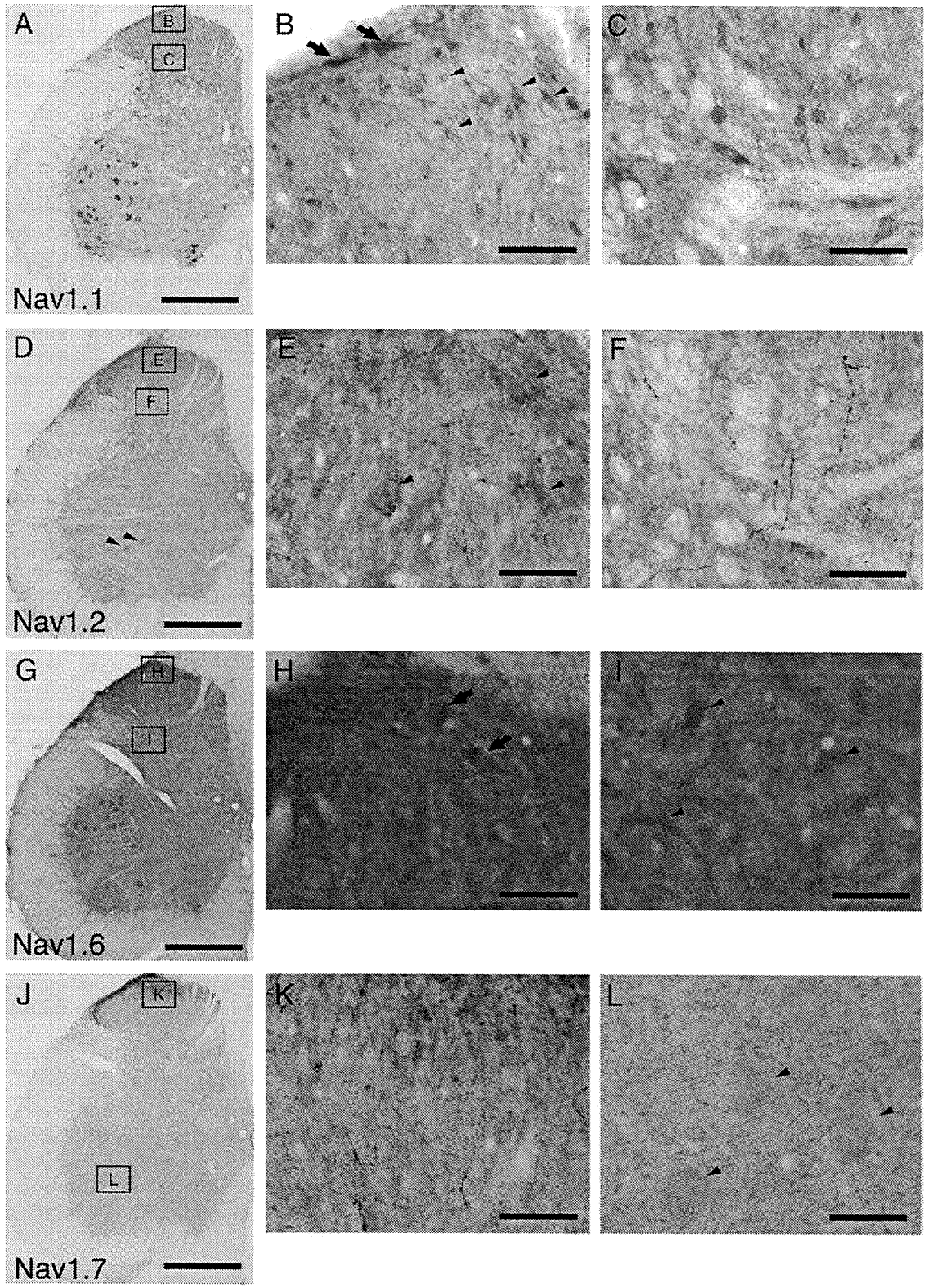

Fig. 5. Immunohistochemistry of Nav1.1 (A–C), Nav1.2 (D–F), Nav1.6 (G–I), and Nav1.7 (J–L) in the rat naïve lumbar spinal cord transverse sections. The positions of the middle and the right-hand panels were indicated in the left-hand panels. For Nav1.1, the whole gray matter was lightly stained, and intensely-stained neurons were identified in ventral horn (arrows in A), lamina I (arrows in B), outer part of lamina II (arrowheads in B), and deeper laminae of dorsal horn (C). For Nav1.2, the spinal gray matter was lightly stained with few moderately-stained motoneurons (arrowheads in D). Among the densely-stained short varicose fibers, some moderately-stained neuron-like profiles were identified in the superficial layers (arrowheads in E). In the deeper layers, while many fine varicose fibers were densely immunostained (F) almost no positive cells were found. For Nav1.6, the spinal gray matter was lightly stained with many moderately-stained motoneurons (G). In addition, some neuron-like cell profiles in lamina I (arrows in H) and deeper layers (arrowhead in I) were moderately stained. For Nav1.7, the superficial layers of the dorsal horn were selectively stained (J). These layers contained many labeled varicose fibers, but not cell profiles (K). The motoneurons were lightly stained at just detectable level (arrowheads in L). Scale bars=500 μm in (A, D, G, J); 50 μm in others.

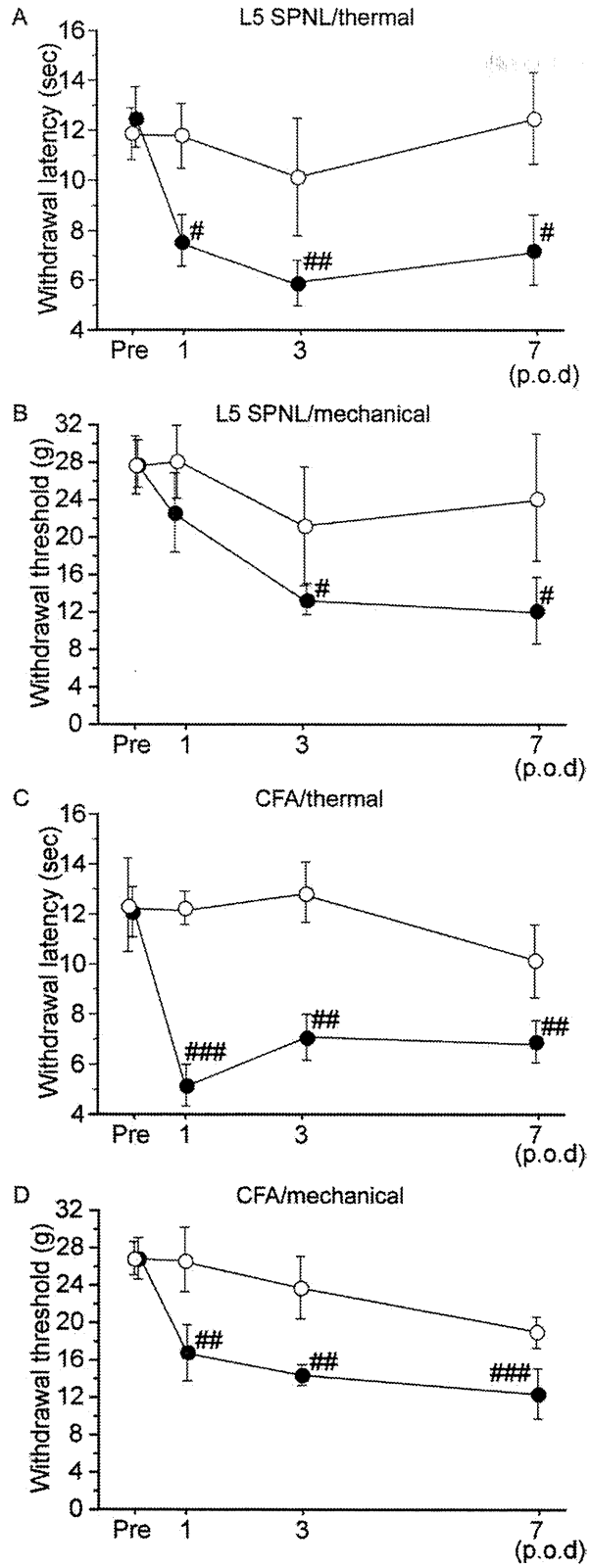

Fig. 6. Pain behavior induced by unilateral L5 spinal nerve ligation (A, B) and intradermal CFA injection to the plantar surface of the hindpaw (C, D). The closed and open circles represent ipsilateral and contralateral side, respectively. Withdrawal latency to radiant heat (thermal; A, C) and withdrawal threshold to increasing pinpoint pressure (mechanical; B, D) to the bilateral plantar surface were measured just before (Pre), and at 1, 3, and 7 post-operative days (p. o. d.). Both groups developed thermal hyperalgesia and mechanical allodynia on the ipsilateral side ($P<0.05$, by repeated measures ANOVA), but not on the contralateral side ($P>0.05$). Note that these behavioral changes continued until 7 p. o. d. when the results from the histochemical studies were examined. $n=4$; error bars=SEM. $^{\#}$ $P<0.05$, $^{\#\#}$ $P<0.01$, $^{\#\#\#}$ $P<0.001$ vs. Pre, by Fisher's post hoc test.

C-fiber neurons completely lack these two subunits and express Nav1.8 and Nav1.9 that are not detected in spinal cord (Fukuoka et al., 2008), the selective blockade of the latter two Navs may achieve selective pain elimination at the peripheral nerve level, too.

Nav proteins in spinal neurons

We demonstrated that spinal neurons in the naive adult rat spinal cord express multiple Nav mRNAs (Fig. 3). Although many immunohistochemical studies have examined about Nav expression in spinal cord, there are few reports that demonstrate the localization of Nav proteins in the neuronal cell bodies, except for the spinal motoneurons. This is largely due to the fact that Nav proteins are highly localized at several parts other than cell bodies of spinal neurons, such as axon initial segment, nodes of Ranvier, and along the myelinated axons (Krzemien et al., 2000; Lindia and Abbadie, 2003; Jarnot and Corbett, 2006; Duflocq et al., 2008). Using commercially available well-characterized antibodies, we observed localization of Nav proteins in some neuron-like cell bodies consistent with our ISHH data; (1) Nav1.1 in lamina I and deeper laminae, including the motoneurons (Fig. 5A–C). (2) Nav1.2 in superficial layers (Fig. 5D–F). (3) Nav1.6 in lamina I and deeper laminae, including the motoneurons (Fig. 5G–I). (4) Exclusive expression of Nav1.7 in the spinal motoneurons (Fig. 5J–L). However, the immunopositive cells (Fig. 5) are much less than the Nav mRNA-expressing cells (Figs. 1 and 2), indicating the high sensitivity of our ISHH methods. These observations suggest that neuronal cell body may have relatively small role in action potential propagation. Of course, it is clear that the neuronal electrophysiological characters are determined by the channel proteins, but not directly by their mRNAs. This is also the case of the real molecular targets of sodium channel blockers. However, it is also the fact that proteins are translated from their transcripts. At least, neurons lacking a Nav transcript could not have the corresponding channel protein in any region of their structural components. Therefore, the laminae-specific neuronal expression of Nav transcripts should indicate some difference in electrophysiological properties of their dendrites and axons of the spinal neurons in these laminae.

L5 SPNL induced a change in Navs expression only in spinal motoneurons

L5 SPNL and chronic constriction injury (CCI) of the sciatic nerve are widely used neuropathic pain models. Dorsal horn neurons exhibit abnormal electrophysiological characters including spontaneous background activity after L5

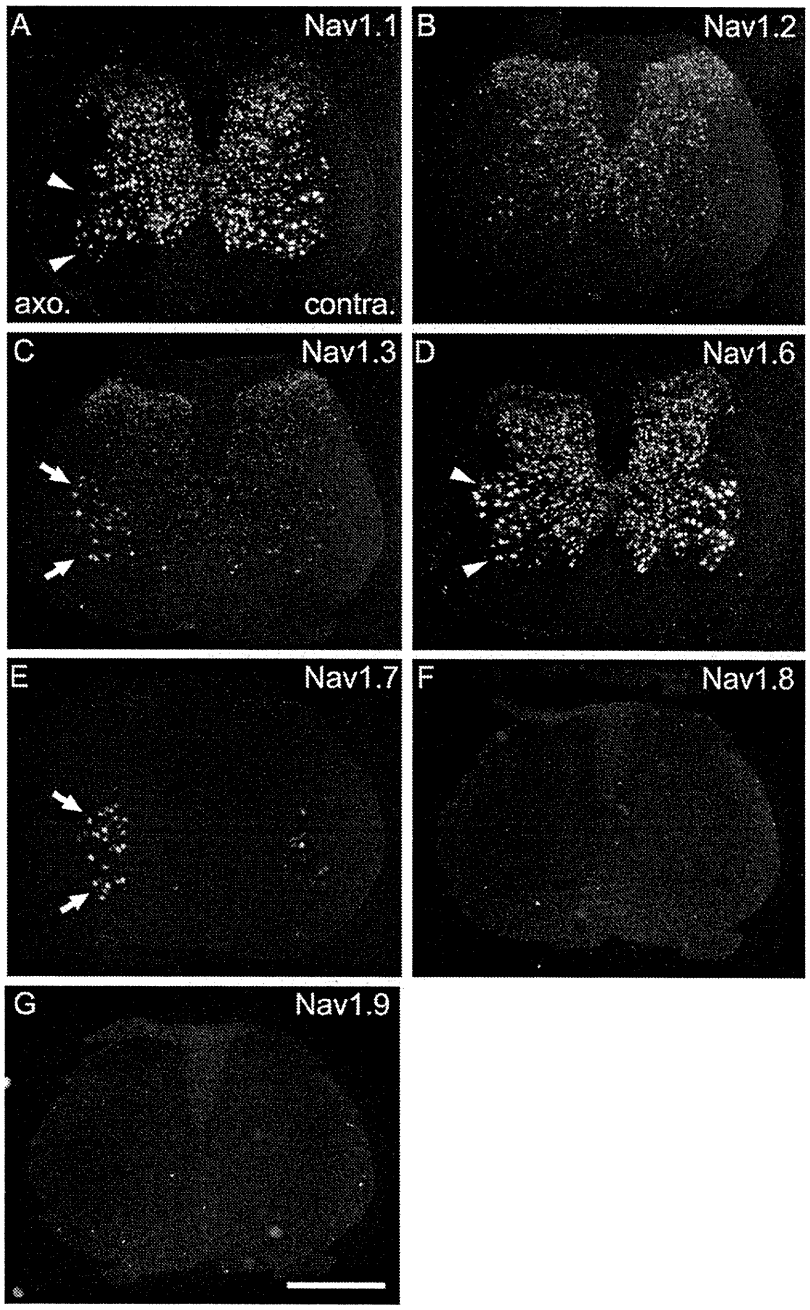

Fig. 7. Darkfield photomicrographs of transverse section of rat L5 lumbar spinal cord showing *in situ* hybridization signals for Nav1.1 (A), Nav1.2 (B), Nav1.3 (C), Nav1.6 (D), Nav1.7 (E), Nav1.8 (F), and Nav1.9 (G) mRNAs 7 d after L5 spinal nerve ligation. The left and right side of each image are the ipsilateral (axo.) and contralateral (contra.) side, respectively. Note that the axotomized spinal motoneurons in the ventral horn slightly decreased Nav1.1 and Nav1.6 mRNAs (arrowheads in A, D), and significantly increased Nav1.3 and Nav1.7 mRNAs (arrows in C, E). No significant differences were observed in the dorsal horn for all Navs. There were no signals for Nav1.8 or 1.9 in any part of the spinal cord. Scale bar, 1 mm.

SPNL (Pertovaara et al., 1997; Suzuki and Dickenson, 2006) and CCI (Laird and Bennett, 1993). Since *de novo* expression of Nav1.3 transcript has been demonstrated in spinal dorsal horn 10 days after CCI (Hains et al., 2004), we examined the change in expression of Navs 7 days after L5 SPNL. Although, we verified the development of mechanical allodynia and thermal hyperalgesia at the time point (Fig. 6), we could not detect any changes of Nav expression in dorsal horn (Fig. 7). Therefore, CCI may involve unknown pathomechanisms that increase this Nav in the spinal cord other than those induced by simple spinal nerve lesion. On the other hand, we found upregulation of Nav1.3 and Nav1.7 and downregulation of Nav1.1 and Nav1.6 in spinal motoneurons (Figs. 7 and 8). Previous studies report the upregulation of Nav1.3 in directly axotomized facial motoneurons (Iwahashi et al., 1994), but not in spinal motoneurons following axotomy resulting from spinal cord injury (Hains et al., 2002). It has been demon-

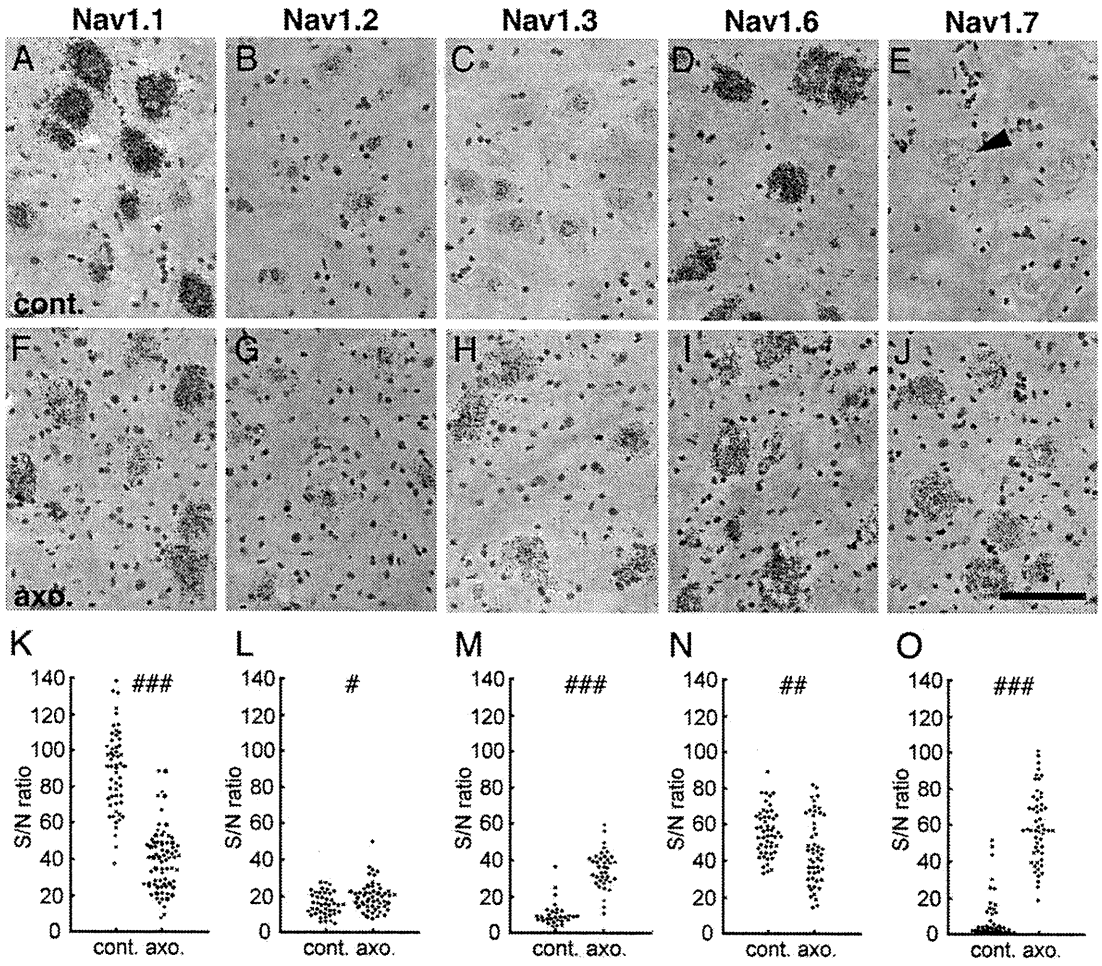

Fig. 8. Axotomy-induced changes of Nav expression in spinal motoneurons. Brightfield photomicrographs of ventral horns of rat L5 lumbar spinal cord showing *in situ* hybridization signals for Nav1.1 (A, F, K), Nav1.2 (B, G, L), Nav1.3 (C, H, M), Nav1.6 (D, I, N), and Nav1.7 (E, J, O) mRNAs 7 days after L5 spinal nerve ligation. The upper and middle panels are the contralateral (cont.) and ipsilateral (axo.) side, respectively. Scale bar, 100 μm. The bottom panels show scatter plots of ISHH signals of individual motoneurons pooled from at least six sections from four rats and the statistical results comparing both sides. $^{\#}P<0.05$, $^{\#\#}P<0.01$, $^{\#\#\#}P<0.001$, by Wilcoxon Signed Rank test. Note the significant decrease of Nav1.1 and Nav1.6, and the increase of Nav1.3 and Nav1.7 mRNAs.

strated that the axotomized spinal motoneurons exhibit a relatively higher frequency of firing (Gustafsson, 1979). The rapid repriming property of Nav1.3 may contribute to this electrophysiological change as suggested in primary afferent neurons (Cummins et al., 2001), while the contribution of the upregulated Nav1.7 is still unclear.

Navs in the spinal cord after CFA-induced inflammation

CFA-induced peripheral inflammation causes electrophysiological changes in second-order sensory neurons, including increased responsiveness, enlargement of receptive field, and increased background activity (Iwata et al., 1999). Of course, some of these changes are caused by central sensitization of spinal neurons (Ren et al., 1996; Guo et al., 2002). On the other hand, intradermal injection of CFA induces upregulation of several sensory-related molecules in dorsal horn neurons, including NK-1 (Ji et al., 2002), NMDA receptor (Ohtori et al., 2002), and ASICs (Wu et al., 2004). The same inflammation, however, did not induce any transcriptional changes of Navs in lumbar spinal neurons. The electrophysiological changes in this pathological state may involve some post-translational modulation of Navs such as phosphorylation and glycosilation (Tyrrell et al., 2001; Vijayaragavan et al., 2004; Wittmack et al., 2005).

CONCLUSION

Spinal neurons possess VGSCs with different composition of α-subunits according to their laminae location. Comparison with our previous data concerning the subpopulation-specific distribution of Nav transcripts in DRG neurons provide the precise distribution of Navs in the spinal cord and peripheral nerves. Selective blockade of some Navs may exert a differential functional influence on sensory transmission and motor function.

Acknowledgments—This work was supported by a Grant-in Aid (Grant No 19603019) from Japanese Ministry of Education, Sci-

ence and Culture (Dr. Fukuoka). We thank Dave. A. Thomas for correcting the English usage.

REFERENCES

Al-Khater KM, Kerr R, Todd AJ (2008) A quantitative study of spinothalamic neurons in laminae I, III, and IV in lumbar and cervical segments of the rat spinal cord. J Comp Neurol 511:1–18.

Black JA, Dib-Hajj S, McNabola K, Jeste S, Rizzo MA, Kocsis JD, Waxman SG (1996) Spinal sensory neurons express multiple sodium channel alpha-subunit mRNAs. Brain Res Mol Brain Res 43:117–131.

Black JA, Liu S, Tanaka M, Cummins TR, Waxman SG (2004) Changes in the expression of tetrodotoxin-sensitive sodium channels within dorsal root ganglia neurons in inflammatory pain. Pain 108:237–247.

Burstein R, Dado RJ, Giesler GJ Jr (1990) The cells of origin of the spinothalamic tract of the rat: a quantitative reexamination. Brain Res 511:329–337.

Craig AD (1995) Distribution of brainstem projections from spinal lamina I neurons in the cat and the monkey. J Comp Neurol 361:225–248.

Cummins TR, Aglieco F, Renganathan M, Herzog RI, Dib-Hajj SD, Waxman SG (2001) Nav1.3 sodium channels: rapid repriming and slow closed-state inactivation display quantitative differences after expression in a mammalian cell line and in spinal sensory neurons. J Neurosci 21:5952–5961.

Dib-Hajj SD, Tyrrell L, Black JA, Waxman SG (1998) NaN, a novel voltage-gated Na channel, is expressed preferentially in peripheral sensory neurons and down-regulated after axotomy. Proc Natl Acad Sci U S A 95:8963–8968.

Duflocq A, Le Bras B, Bullier E, Couraud F, Davenne M (2008) Nav1.1 is predominantly expressed in nodes of Ranvier and axon initial segments. Mol Cell Neurosci 39:180–192.

Felts PA, Yokoyama S, Dib-Hajj S, Black JA, Waxman SG (1997) Sodium channel alpha-subunit mRNAs I, II, III, NaG, Na6 and hNE (PN1): different expression patterns in developing rat nervous system. Brain Res Mol Brain Res 45:71–82.

Fukuoka T, Kondo E, Dai Y, Hashimoto N, Noguchi K (2001) Brain-derived neurotrophic factor increases in the uninjured dorsal root ganglion neurons in selective spinal nerve ligation model. J Neurosci 21:4891–4900.

Fukuoka T, Kobayashi K, Yamanaka H, Obata K, Dai Y, Noguchi K (2008) Comparative study of the distribution of the alpha-subunits of voltage-gated sodium channels in normal and axotomized rat dorsal root ganglion neurons. J Comp Neurol 510:188–206.

Garcia KD, Sprunger LK, Meisler MH, Beam KG (1998) The sodium channel Scn8a is the major contributor to the postnatal developmental increase of sodium current density in spinal motoneurons. J Neurosci 18:5234–5239.

Goldin AL, Barchi RL, Caldwell JH, Hofmann F, Howe JR, Hunter JC, Kallen RG, Mandel G, Meisler MH, Netter YB, Noda M, Tamkun MM, Waxman SG, Wood JN, Catterall WA (2000) Nomenclature of voltage-gated sodium channels. Neuron 28:365–368.

Guo W, Zou S, Guan Y, Ikeda T, Tal M, Dubner R, Ren K (2002) Tyrosine phosphorylation of the NR2B subunit of the NMDA receptor in the spinal cord during the development and maintenance of inflammatory hyperalgesia. J Neurosci 22:6208–6217.

Gustafsson B (1979) Changes in motoneurone electrical properties following axotomy. J Physiol 293:197–215.

Hains BC, Black JA, Waxman SG (2002) Primary motor neurons fail to up-regulate voltage-gated sodium channel Na(v)1.3/brain type III following axotomy resulting from spinal cord injury. J Neurosci Res 70:546–552.

Hains BC, Saab CY, Klein JP, Craner MJ, Waxman SG (2004) Altered sodium channel expression in second-order spinal sensory neurons contributes to pain after peripheral nerve injury. J Neurosci 24:4832–4839.

Iwahashi Y, Furuyama T, Inagaki S, Morita Y, Takagi H (1994) Distinct regulation of sodium channel types I, II and III following nerve transection. Brain Res Mol Brain Res 22:341–345.

Iwata K, Tashiro A, Tsuboi Y, Imai T, Sumino R, Morimoto T, Dubner R, Ren K (1999) Medullary dorsal horn neuronal activity in rats with persistent temporomandibular joint and perioral inflammation. J Neurophysiol 82:1244–1253.

Jarnot M, Corbett AM (2006) Immunolocalization of NaV1.2 channel subtypes in rat and cat brain and spinal cord with high affinity antibodies. Brain Res 1107:1–12.

Jarvis MF, Honore P, Shieh CC, Chapman M, Joshi S, Zhang XF, Kort M, Carroll W, Marron B, Atkinson R, Thomas J, Liu D, Krambis M, Liu Y, McGaraughty S, Chu K, Roeloffs R, Zhong C, Mikusa JP, Hernandez G, Gauvin D, Wade C, Zhu C, Pai M, Scanio M, Shi L, Drizin I, Gregg R, Matulenko M, Hakeem A, Gross M, Johnson M, Marsh K, Wagoner PK, Sullivan JP, Faltynek CR, Krafte DS (2007) A-803467, a potent and selective Nav1.8 sodium channel blocker, attenuates neuropathic and inflammatory pain in the rat. Proc Natl Acad Sci U S A 104:8520–8525.

Ji RR, Befort K, Brenner GJ, Woolf CJ (2002) ERK MAP kinase activation in superficial spinal cord neurons induces prodynorphin and NK-1 upregulation and contributes to persistent inflammatory pain hypersensitivity. J Neurosci 22:478–485.

Kim SH, Chung JM (1992) An experimental model for peripheral neuropathy produced by segmental spinal nerve ligation in the rat. Pain 50:355–363.

Kobayashi Y (1998) Distribution and morphology of spinothalamic tract neurons in the rat. Anat Embryol (Berl) 197:51–67.

Krzemien DM, Schaller KL, Levinson SR, Caldwell JH (2000) Immunolocalization of sodium channel isoform NaCh6 in the nervous system. J Comp Neurol 420:70–83.

Laird JM, Bennett GJ (1993) An electrophysiological study of dorsal horn neurons in the spinal cord of rats with an experimental peripheral neuropathy. J Neurophysiol 69:2072–2085.

Lindia JA, Abbadie C (2003) Distribution of the voltage gated sodium channel Na(v)1.3-like immunoreactivity in the adult rat central nervous system. Brain Res 960:132–141.

Menetrey D, Chaouch A, Binder D, Besson JM (1982) The origin of the spinomesencephalic tract in the rat: an anatomical study using the retrograde transport of horseradish peroxidase. J Comp Neurol 206:193–207.

Novakovic SD, Tzoumaka E, McGivern JG, Haraguchi M, Sangameswaran L, Gogas KR, Eglen RM, Hunter JC (1998) Distribution of the tetrodotoxin-resistant sodium channel PN3 in rat sensory neurons in normal and neuropathic conditions. J Neurosci 18:2174–2187.

Ohtori S, Takahashi K, Ino H, Chiba T, Yamagata M, Sameda H, Moriya H (2002) Up-regulation of substance P and NMDA receptor mRNA in dorsal horn and preganglionic sympathetic neurons during adjuvant-induced noxious stimulation in rats. Ann Anat 184: 71–76.

Paxinos G, Watson C (1986) The rat brain in stereotaxic coordinates, 2nd edition. CA: Elsevier Academic Press.

Pertovaara A, Kontinen VK, Kalso EA (1997) Chronic spinal nerve ligation induces changes in response characteristics of nociceptive spinal dorsal horn neurons and in their descending regulation originating in the periaqueductal gray in the rat. Exp Neurol 147:428–436.

Planells-Cases R, Caprini M, Zhang J, Rockenstein EM, Rivera RR, Murre C, Masliah E, Montal M (2000) Neuronal death and perinatal lethality in voltage-gated sodium channel alpha(II)-deficient mice. Biophys J 78:2878–2891.

Porter JD, Goldstein LA, Kasarskis EJ, Brueckner JK, Spear BT (1996) The neuronal voltage-gated sodium channel, Scn8a, is essential for postnatal maturation of spinal, but not oculomotor, motor units. Exp Neurol 139:328–334.

Ren K, Iadarola MJ, Dubner R (1996) An isobolographic analysis of the effects of N-methyl-D-aspartate and NK1 tachykinin receptor